SUPPORTING ONLINE MATERIAL FOR

# Bookmarking promoters in mitotic chromatin: Poly(ADP-ribose)Polymerase-1 as an epigenetic mark

Niraj Lodhi, Andrew V. Kossenkov and Alexei V. Tulin

**This file includes:**

SI Figures S1 – S8.

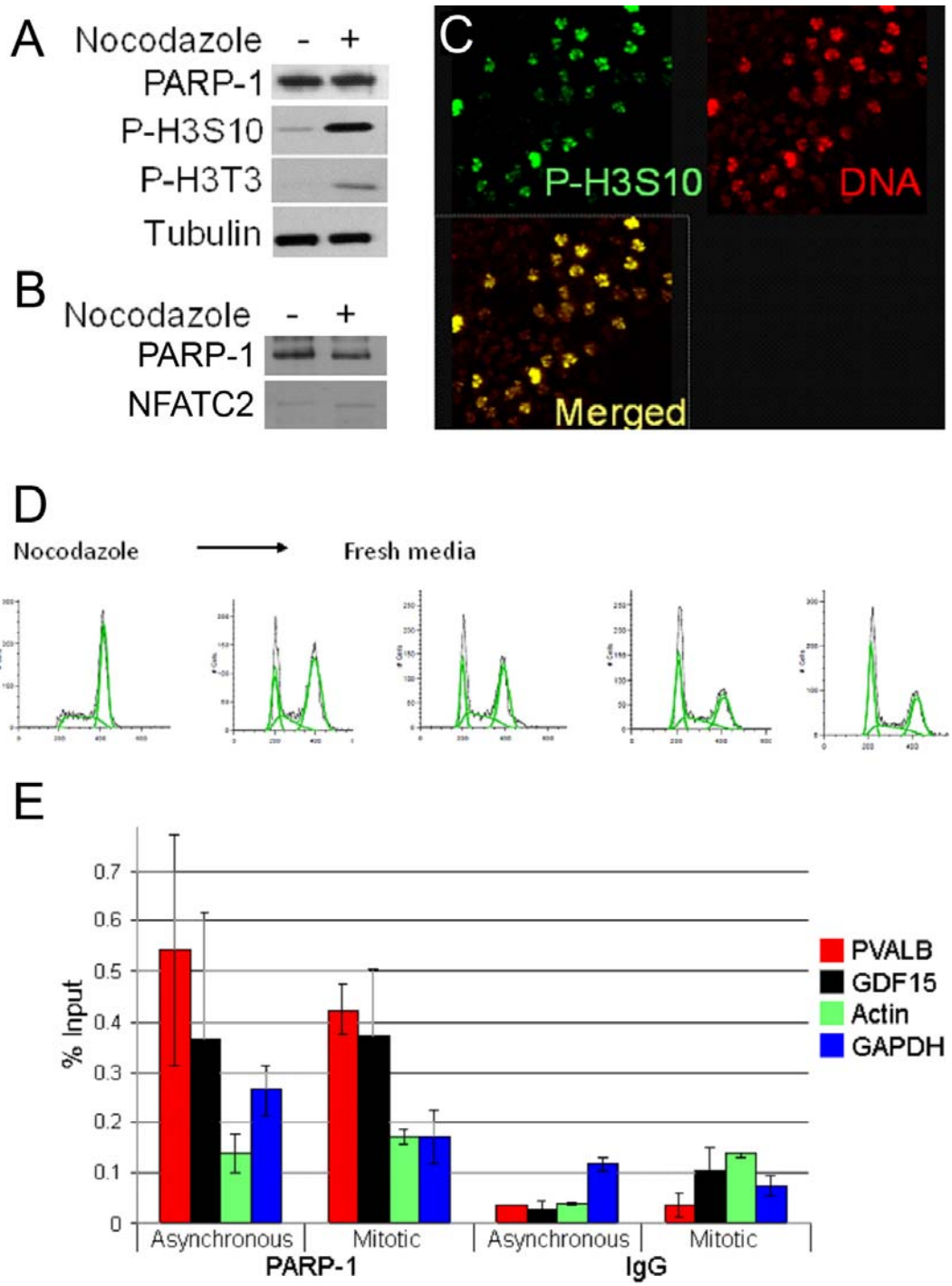


**Figure S1 (related to Figure 1). PARP-1 remained in chromatin during mitosis. A.** Equal amounts of total proteins extracted from asynchronous cells and cells arrested in mitosis were analyzed after PAGE on Western blot using anti-PARP-1, anti-phospho-Ser10-H3 (a marker of mitotic chromatin), anti-phospho histone H3 threonine 3 (H3-T3), and anti-α tubulin antibodies. **B.** Total nuclear PARP-1 and NFATC2 proteins correspond to equal DNA amouns. **C.** Confocal microscopy of cells synchronized in mitosis by nocodazole treatment. To detect cells in mitosis, the antibody against the mitotic chromatin marker phospho-Ser10-H3 was used (green). Draq5 staining reveals DNA (red). 99% of cells demonstrate precise arrest in metaphase (yellow). **D.** Nocodazole treatment does not affect cell viability. FACS analysis demonstrates that cells synchronously enter the next cell cycle upon nocodazole removal. **E.** PARP-1 occupies genomic sites in the PARP-1-dependent loci PVALB and GDF15, but not in GAPDH or Actin. Comparative ChIP assays using anti-PARP-1 and control IgG antibodies.

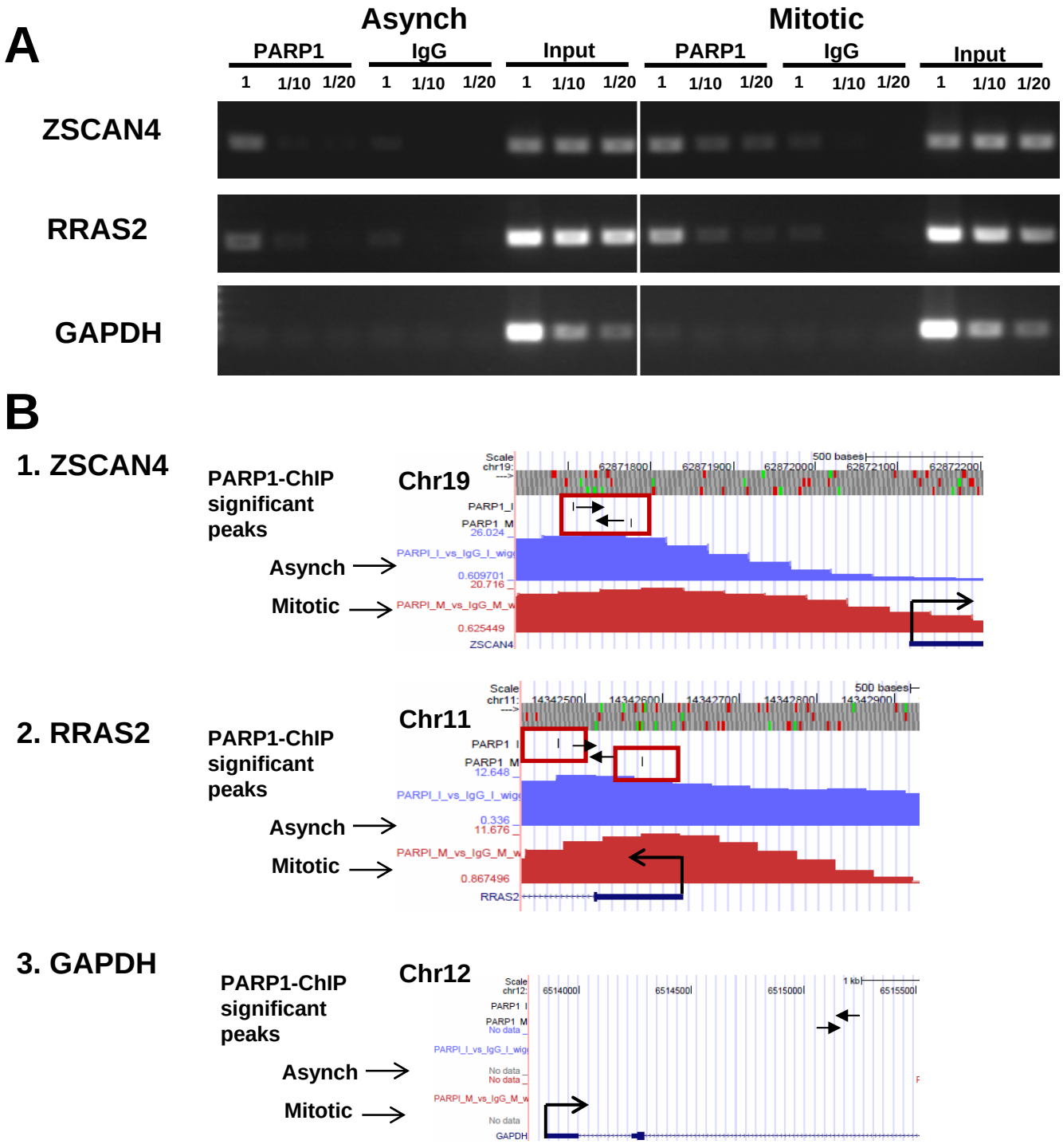


**Figure S2 (related to Figure 1). Comparative ChIP-PCR in serial dilution to validate PARP-1 binding to genes.** The validation of ChIP-seq results, using the conventional ChIP assay for PARP-1 occupied loci ZSCAN4 (**1**) and RRAS2 (**2**), along with PARP-1 negative GAPDH locus (**3**). UCSC genome browser view is presented from ChIP-Seq data (below). **A**. ChIP-PCR in serial dilution showing enrichment of PARP-1 in comparison to nonspecific control IgG for ZSCAN4 and RRAS2 in asynchronous and mitotic conditions and no PARP-1 enrichment in GAPDH ChIP-PCR. **B**. ChIP-seq tracks showing locations of PARP-1 on promoters of ZSCAN4 and RRAS2 genes in asynchronous and mitotic chromatin and no PARP-1 presence on GAPDH gene. Red box represents the area of chromatin tested in conventional ChIP assay. Arrows in red boxes indicate positions of primers for ChIP-PCR around PARP-1 binding. Black arrow indicates the location and direction of transcription.

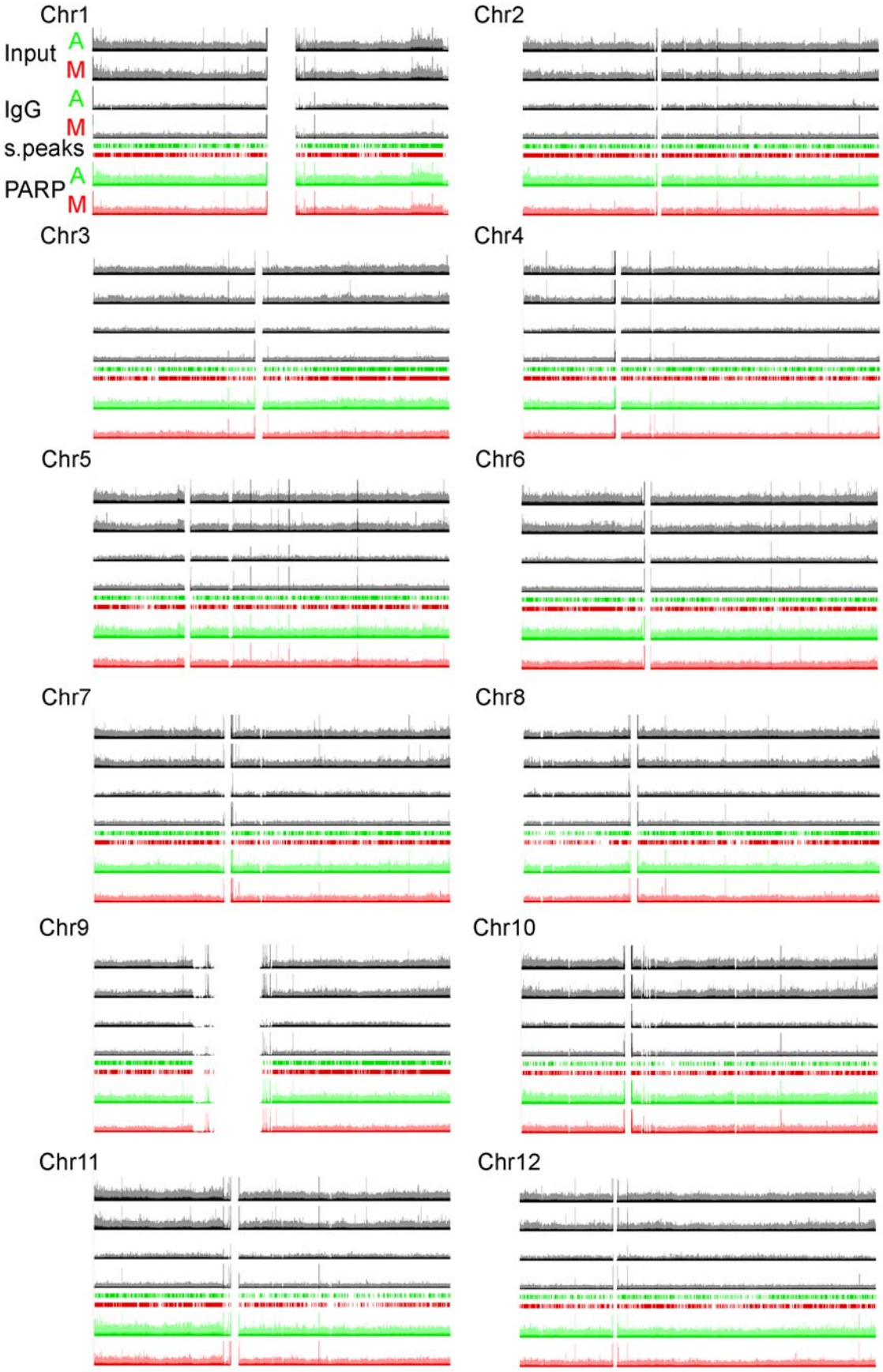


**Figure S3 (related to Figure 2).** The chromosomal level of PARP-1 binding in mitotic (M) and asynchronous cells. Chromosomes 1 – 12. s.peaks – significant peaks.

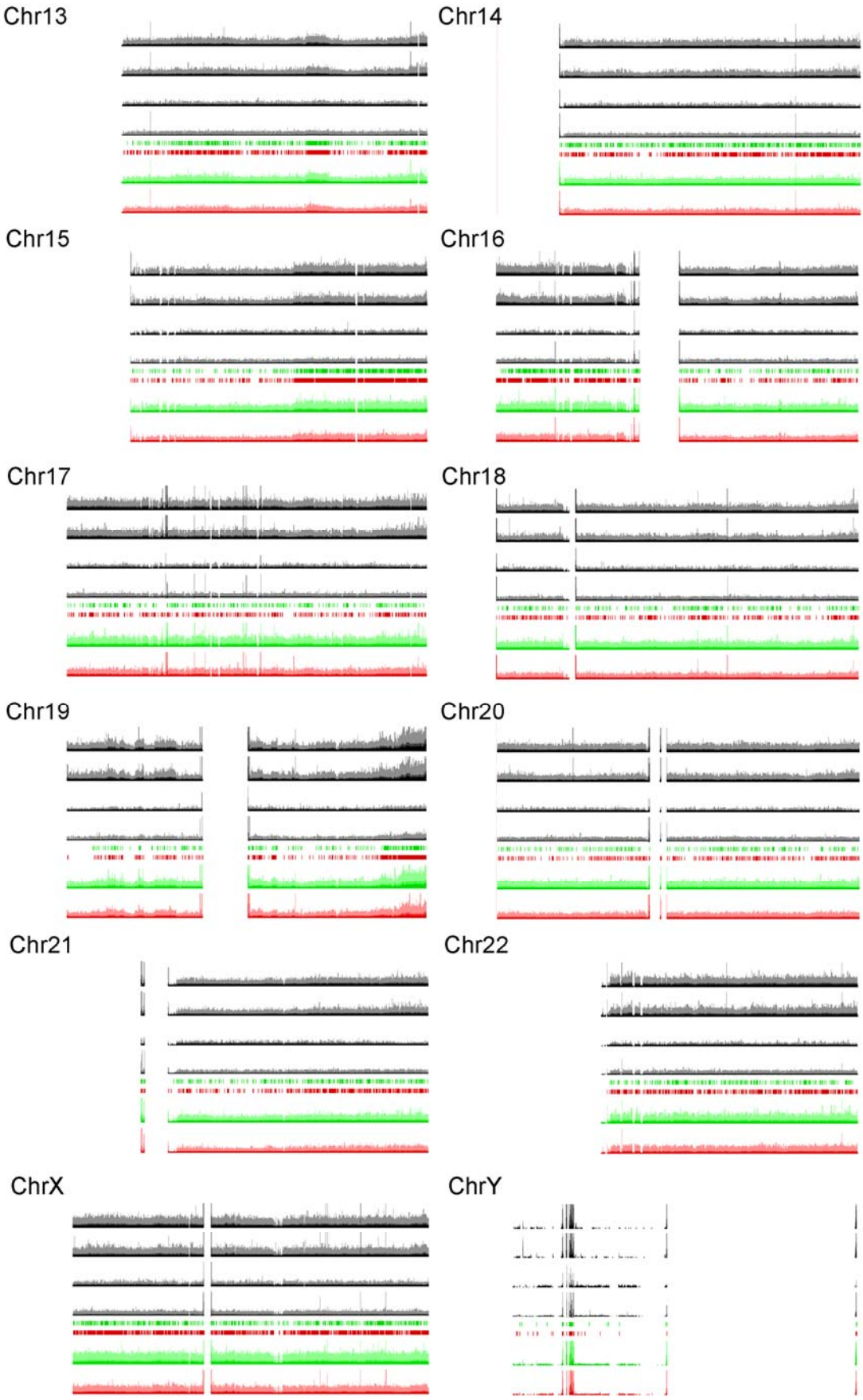


**Figure S4 (related to Figure 2).** The chromosomal level of PARP-1 binding in mitotic (M) and asynchronous cells. Chromosomes 13 – Y.

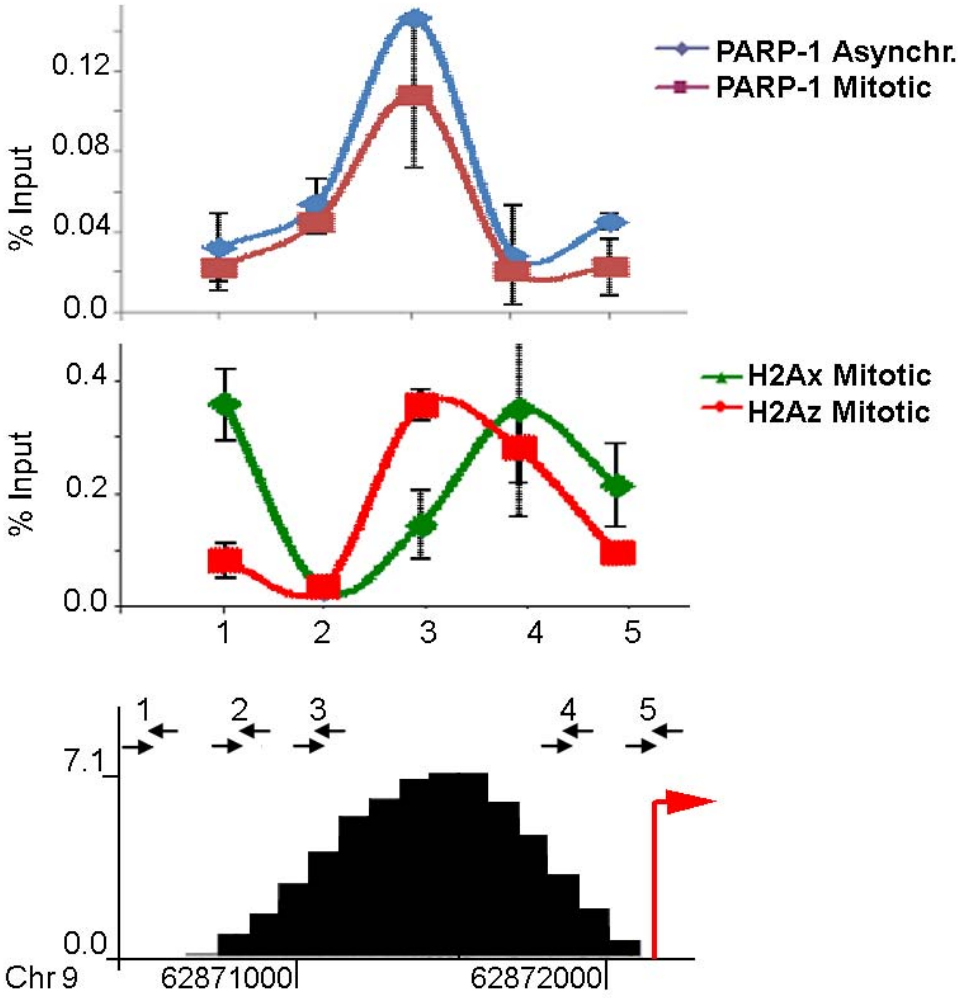


**Figure S5 (related to Figure 3). PARP-1 binding site within ZSCAN4 locus colocalizes with H2A.Z/H2AX histones.** Arrows indicate positions of oligonucleotide primers along human genome sequence which were used in ChIP assay (**top**) and ChIP-seq PARP-1 pick (**bottom**).

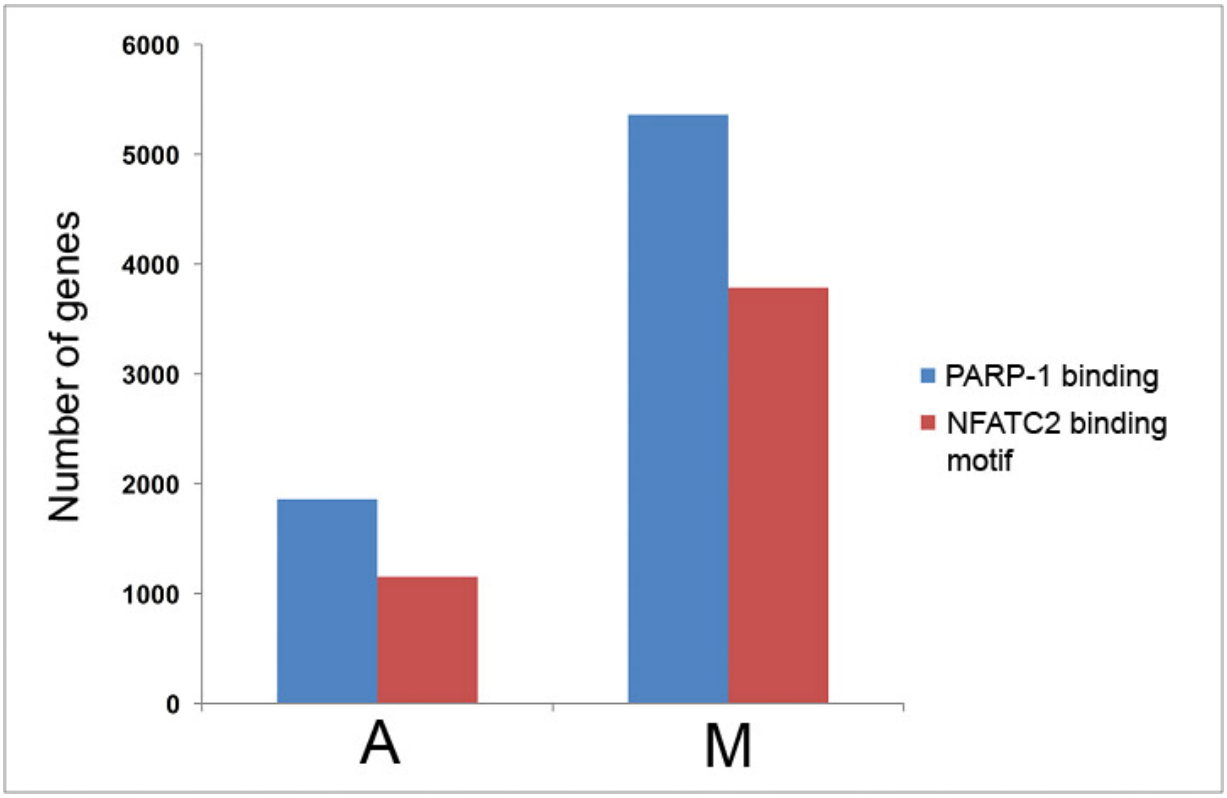


**Figure S6 (related to Figure 4). PARP-1 binding sites co-occur with NFATC2 binding consensus.** Consensus binding motif found in proximity to PARP-1 binding sites. The most significant motifs associated with PARP-1 binding sites in mitotic (M) and asynchronized (A) cells were compared to known NFATC2 binding motif.

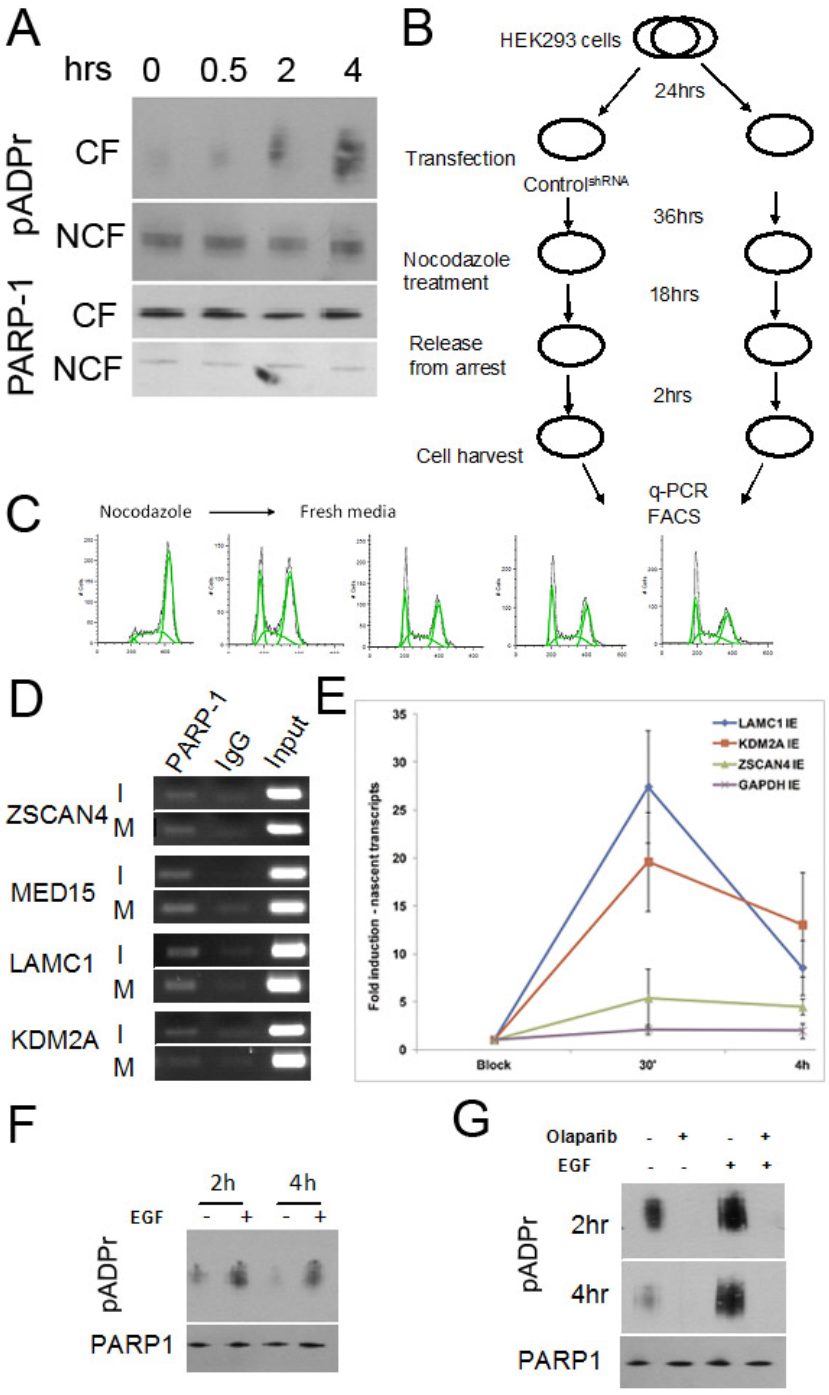


**Figure S7 (related to Figure 6). PARP-1 protein and its enzymatic activity are required to restart post-mitotic transcription.** **A.** Poly(ADP-ribose) accumulates in chromatin after mitosis. **B.** shRNA approach to PARP-1 knockdown. HEK cells (5x105 cells) were seeded on 60mm plates for 24 hrs. At 70% confluence, cells were transfected with shRNA control and shRNAPARP-1 using Effectene (Qiagen) for 36 hrs. Cells were washed two times with PBS and treated with nocodazole (100ng/ml) for 18hrs. After washing two times with PBS, synchronized cells were released in a time-dependent manner (0, 1:30, 2:30, 4 and 5:30 hrs). PARP-1 knockdown was checked using qPCR for primary transcript detection and FACS analysis at each time point. **C.** PARP-1 shRNA knockdown does not affect cell cycle progression. As demonstrated by FACS analysis, cells synchronously enter the next cell cycle upon nocodazole removal in control and PARP-1 shRNA-treated cells. D. ChIP-PCR showing enrichment of PARP-1 in comparison to nonspecific control IgG for ZSCAN4, MED15, LAMC1 and KDM2A loci in asynchronous (I) and mitotic (M) conditions. **E.** Newly transcribed RNA (IE) can not be detected during mitosis (block). Data show that IE RNA amount is rapidly increasing post mitotically for PARP-1-dependent genes, but slowly for a PARP-1-independent gene (GAPDH). **F.** EGF treatment stimulates pADPr in postmitotic chromatin. **G.** Olaparib inhibits EGF-dependent pADP-ribosylation.

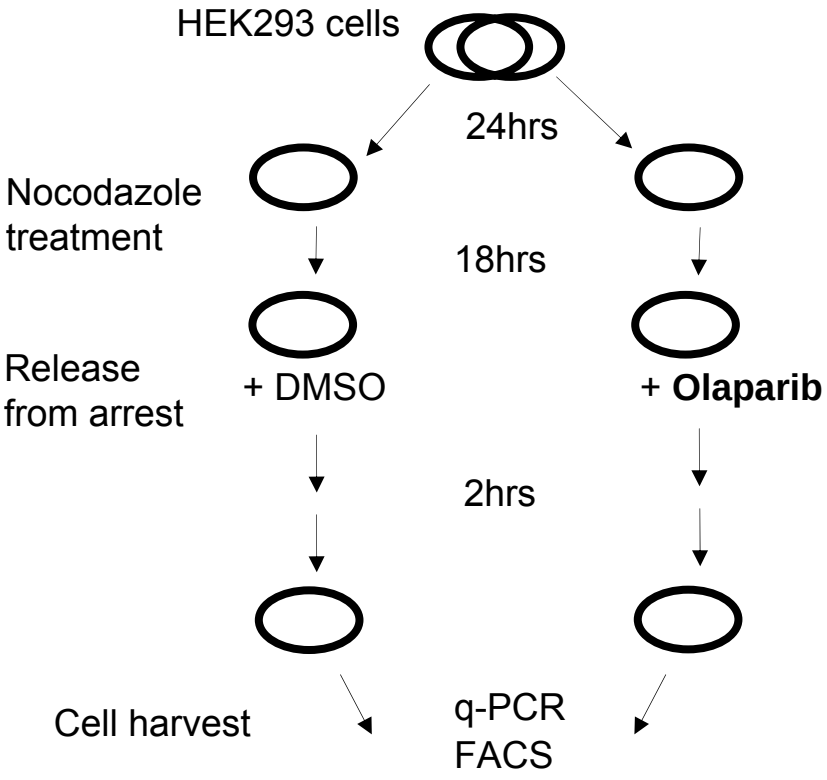


**Figure S8 (related to Figure 6). PARP-1 enzymatic activity is required to restart post-mitotic transcription.** Diagram illustrating PARP-1 inhibition approach. To check the primary transcript after Olaparib treatment, HEK cells (5x105) were seeded on 60mm plates for 24 hrs. At 70% confluence, cells were treated with nocodazole (100ng/ml) for 18hrs. After washing two times with PBS, synchronized cells were released in presence and absence of Olaparib in a time-dependent manner (0, 1:30, 2:30, 4 and 5:30 hrs). Cells were quickly harvested to isolate total RNA for qPCR and FACS analysis. Primary transcript of selected genes was quantified at 2hrs after release of cells.